

Extended (Conventional) Co-Prime Arrays and Difference Set Analysis: Low Latency Approach

Usham V. Dias

Department of Electrical Engineering, Indian Institute of Technology Delhi, India.

Abstract—The co-prime array is a sub-Nyquist acquisition scheme for the estimation of second order statistics. It cannot generate all the difference values in the co-prime range and hence, one of the sub-array is extended to enable the estimation of the second order statistics at each difference value in the co-prime range. Recently, the difference set for the co-prime array was studied and low latency temporal spectrum estimation was demonstrated. In this paper, the fundamentals of the difference set of the extended co-prime array, also known as the conventional co-prime array, is developed. The closed-form equations for the weight function, correlogram bias window, and the variance are described. This is provided for the entire difference set, continuous difference set and for the prototype co-prime period. It is shown that the choice of $M \approx \frac{N}{2}$ generates a bias function with a large relative amplitude between the main-lobe and side-lobe peaks, where M and N are co-prime pairs. The expressions for the number of multiplications and additions required to compute the autocorrelation for the entire, continuous, and prototype range is derived. Simulation results demonstrate low latency spectrum estimation using the correlogram method.

Index Terms—Autocorrelation, spectrum, sparse, co-prime, low latency.

I. INTRODUCTION

CO-PRIME sensing scheme provides a framework for sub-Nyquist acquisition and estimation of the second order statistics of a signal [1]. It has several applications which include direction of arrival estimation [2]–[5], power spectrum estimation [6], [7], system identification [8], beamforming [9]–[11], cross-correlation estimation, time-delay, range, velocity, and acceleration estimation [12].

Low latency co-prime estimation was reported for modal analysis [13] and frequency estimation [14], [15]. A detailed analysis of correlogram spectral estimation method with low latency is considered in [16]. It will form the basis for the discussions on autocorrelation and correlogram estimation in this paper.

However, the co-prime array cannot generate a difference set containing all the elements in the co-prime range $[-MN + 1, MN - 1]$ and hence, an extended co-prime array was proposed in [17]. It has one of the sub-arrays extended by an additional co-prime period. The extended co-prime array generates all the values in the co-prime range but this range does not represent the largest continuous range. The weight function of the extended co-prime array is given in Table IV of [18] for $M = 4$ and $N = 5$, but does not provide a general expression for arbitrary values of M and N . This paper develops the fundamentals of the difference set for the extended (also known as conventional) co-prime

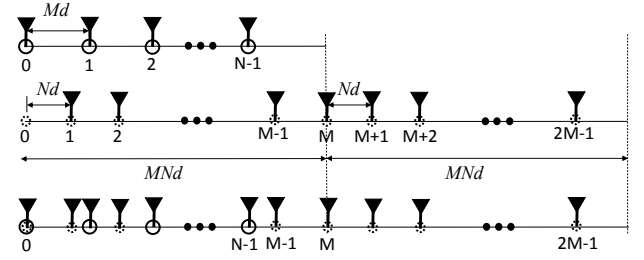


Fig. 1: Extended co-prime structure

array and demonstrates low latency estimation. The closed-form expressions for the weight function and the bias window for the correlogram method are also provided. It may be noted that both the samplers (instead of only one) can be extended for two or more periods. This concept is referred to as the prototype co-prime sampling with multiple periods and is well studied for low latency estimation [16].

II. EXTENDED CO-PRIME CONCEPT

An extended co-prime array is shown in Fig. 1 where M and N are co-prime. The Nyquist distance between the antennas is denoted by d . It has two sub-arrays and the antenna locations are given by:

$$\begin{aligned} P1 &= \{Mnd, 0 \leq n \leq N - 1\} \\ P2 &= \{Nmd, 0 \leq m \leq 2M - 1\} \end{aligned}$$

Note that the antenna at the zeroth location is common to both the sub-arrays. In this paper, we assume that the second array with inter-element spacing of Nd is extended. However, the first array could have been extended, without affecting the concept that governs this scheme. In the temporal or spacial domain, one prototype co-prime period is $[0, MN - 1]$ while the extended co-prime period is $[0, 2MN - 1]$. It may be noted that the co-prime and extended co-prime range that corresponds to one period for autocorrelation (or other second order statistics) is $[-(MN - 1), MN - 1]$ and $[-(2MN - 1), 2MN - 1]$ respectively. Fig. 2 describes this concept from a sampling perspective. Here d represents the Nyquist sampling period. The structure implies that one of the sampler is turned off every alternate co-prime period, while the other sampler uniformly samples the incoming signal. Every extended co-prime period is referred to as a snapshot. The second order statistics (e.g. autocorrelation, power spectrum, etc.) is estimated for each snapshot. Averaging across several

TABLE I: Summary of unique differences (or *dof*) per difference set

Set	\mathbf{L}_{SM}^+	\mathbf{L}_{SM}^-	\mathbf{L}_{SN}^+	\mathbf{L}_{SN}^-	\mathbf{L}_S^+	\mathbf{L}_S^-	\mathbf{L}_S	\mathbf{L}_C^+	\mathbf{L}_C^-	\mathbf{L}_C
# Unique diffs. (Extended)	N	N	$2M$	$2M$	$2M + N - 1$	$2M + N - 1$	$2(2M + N - 1) - 1$	$2MN$	$2MN$	$3MN + M - N$
# Unique diffs. (Prototype)	N	N	M	M	$M + N - 1$	$M + N - 1$	$2(M + N - 1) - 1$	MN	MN	$MN + M + N - 2$

co-prime array had holes in the co-prime range, while the extended co-prime array generates all the difference values in the co-prime range $[-MN + 1, MN - 1]$. However, it does not represent the maximum continuous range of the extended co-prime array. We present Proposition I which provides the expressions for the range of integers in the cross difference sets of an extended co-prime array and their continuity (i.e. the range without holes). The proposition holds for one extended co-prime period $[0, 2MN - 1]$ with $0 \leq n \leq N - 1$ and $0 \leq m \leq 2M - 1$.

Proposition I:

- 1) \mathbf{L}_C^+ has $2MN$ distinct integers in the range $-N(2M - 1) \leq l_c \leq M(N - 1)$
- 2) \mathbf{L}_C^- has $2MN$ distinct integers in the range $-M(N - 1) \leq l_c \leq N(2M - 1)$
- 3) \mathbf{L}_C^+ has consecutive integers in the range $-(MN + M - 1) \leq l_c \leq N - 1$
- 4) \mathbf{L}_C^- has consecutive integers in the range $-(N - 1) \leq l_c \leq (MN + M - 1)$
- 5) \mathbf{L}_C has consecutive integers in the range $-(MN + M - 1) \leq l_c \leq (MN + M - 1)$ which implies that this set has its first hole at $|l_c| = (MN + M)$.

Proposition I-(1) and I-(2) can be easily proved by substituting the values of n and m in $(Mn - Nm)$ and $(Nm - Mn)$ respectively, to generate the maximum and minimum values in the set.

Proof of Proposition I-(3): Let $l_c = Mn - Nm$ be an element in set \mathbf{L}_C^+ satisfying $-(MN + M - 1) \leq l_c \leq N - 1$. Since $n \in [0, N - 1]$, the range of Mn is $0 \leq Mn \leq M(N - 1)$. Using the range of Mn and l_c , we need to prove that $m \in [0, 2M - 1]$, from the equation $Nm = Mn - l_c$. Therefore:

$$\begin{aligned} -(N - 1) &\leq Nm \leq M(N - 1) + (MN + M - 1) \\ -1 &< m < 2M \\ 0 &\leq m \leq 2M - 1 \end{aligned}$$

which satisfies the required range. Proposition I-(4) can be proved along similar lines as Proposition I-(3).

Proof of Proposition I-(5): Let $l_c = \pm(Mn - Nm)$ be an element in the set \mathbf{L}_C satisfying: $-(MN + M - 1) \leq l_c \leq (MN + M - 1)$, where $m \in [0, 2M - 1]$ and $n \in [0, N - 1]$. First we need to prove that $\pm(MN + M)$ is indeed a hole and then show that the range $-(MN + M - 1) \leq l_c \leq (MN + M - 1)$ is continuous. To prove that $\pm(MN + M)$ is a hole in the set \mathbf{L}_C , it is sufficient to prove that it is a hole in \mathbf{L}_C^+ . This holds true because \mathbf{L}_C^- is a flipped version of \mathbf{L}_C^+ and $\mathbf{L}_C = \mathbf{L}_C^+ \cup \mathbf{L}_C^-$. Let $l_c = Mn - Nm$ be an element in set \mathbf{L}_C^+ , and let us assume that $\pm(MN + M)$ is not a hole and exists in set \mathbf{L}_C^+ . This implies that: $Mn - Nm = \pm(MN + M)$ or $M(n \mp 1) = N(m \pm M)$, hence: $\frac{M}{N} = \frac{(m \pm M)}{(n \mp 1)}$. Since $n - 1 < N$ and $m - M < M$, the ratios $\frac{(m+M)}{(n-1)}$ and $\frac{(m-M)}{(n+1)}$ cannot be satisfied. The proof of continuity in the range $-(MN + M -$

$1) \leq l_c \leq (MN + M - 1)$ follows directly from Proposition I-(3) and I-(4).

IV. WEIGHT FUNCTION

Proposition III in [15] gives the expression for the weight function or the number of sample pairs that contribute to estimate the autocorrelation at each value in the difference set. This parameter affects the convergence, accuracy, latency and bias of the estimate. In this section we present the number of sample pairs that contribute to estimate the autocorrelation for the extended co-prime array and is given as Proposition II.

Proposition II: Let $z(l)$ denote the number of elements contributing to the estimation at difference value l .

- 1) For $l \in \mathbf{L}_{SM}^+ \cup \mathbf{L}_{SM}^- - \{0\}$:

$$z(l) = (N - i) + 1, \{1 \leq i \leq N - 1, l = \pm Mi\}$$

- 2) For $l \in \mathbf{L}_{SN}^+ \cup \mathbf{L}_{SN}^- - \{0\}$:

$$z(l) = (2M - i), \{1 \leq i \leq 2M - 1, l = \pm Ni\}$$

- 3) For $l \in \{l = 0\}$: $z(l) = 2M + N - 1$

- 4) For $l \in \mathbf{L}_C - \mathbf{L}_S$:

$$z(l) = 2, \{l \in \{\mathbf{L}_A^+ \cup \mathbf{L}_A^-\} - \mathbf{L}_S\}$$

$$z(l) = 1, \{l \in \{\mathbf{L}_B^+ \cup \mathbf{L}_B^-\} - \mathbf{L}_S\}$$

It is easy to conclude that the number of sample pairs that map to each difference value in the self difference set of signal $x(Mn)$ is given by $N - i$ as shown in Fig. 3(a). In addition, the cross difference set also has pairs of samples that contribute to the estimate at these self differences except at '0'. Thus justifying Proposition II-(1). Proposition II-(2) can be easily inferred from Fig. 3(b). The number of contributors at difference value '0', Proposition II-(3), is the sum of the contributors of the self difference set of the two arrays at zero minus one pair which is common to both the self difference sets. \mathbf{L}_A^+ and \mathbf{L}_A^- represent the cross difference set of the prototype co-prime array and Proposition III-(4) in [15] shows that $z(l) = 2$ for $\{l \in \{\mathbf{L}_A^+ \cup \mathbf{L}_A^-\} - \mathbf{L}_S\}$. On the other hand, we can establish that $z(l) = 1$ for $\{l \in \{\mathbf{L}_B^+ \cup \mathbf{L}_B^-\} - \mathbf{L}_S\}$ from Fig. 4 and Property I. In Fig. 5 and 6, we provide some examples of the weight function of the extended co-prime array for $M > N$ and $N > M$ respectively. These cases of M and N will also be used as examples for the bias analysis. The weight function forms the basis for the bias and variance analysis of the correlogram spectral estimate of the extended co-prime array.

V. BIAS ANALYSIS

The fundamentals of the correlogram method for co-prime based spectral estimation was developed in [16]. This section derives the bias of the correlogram spectral estimate for the extended co-prime array for the entire difference set,

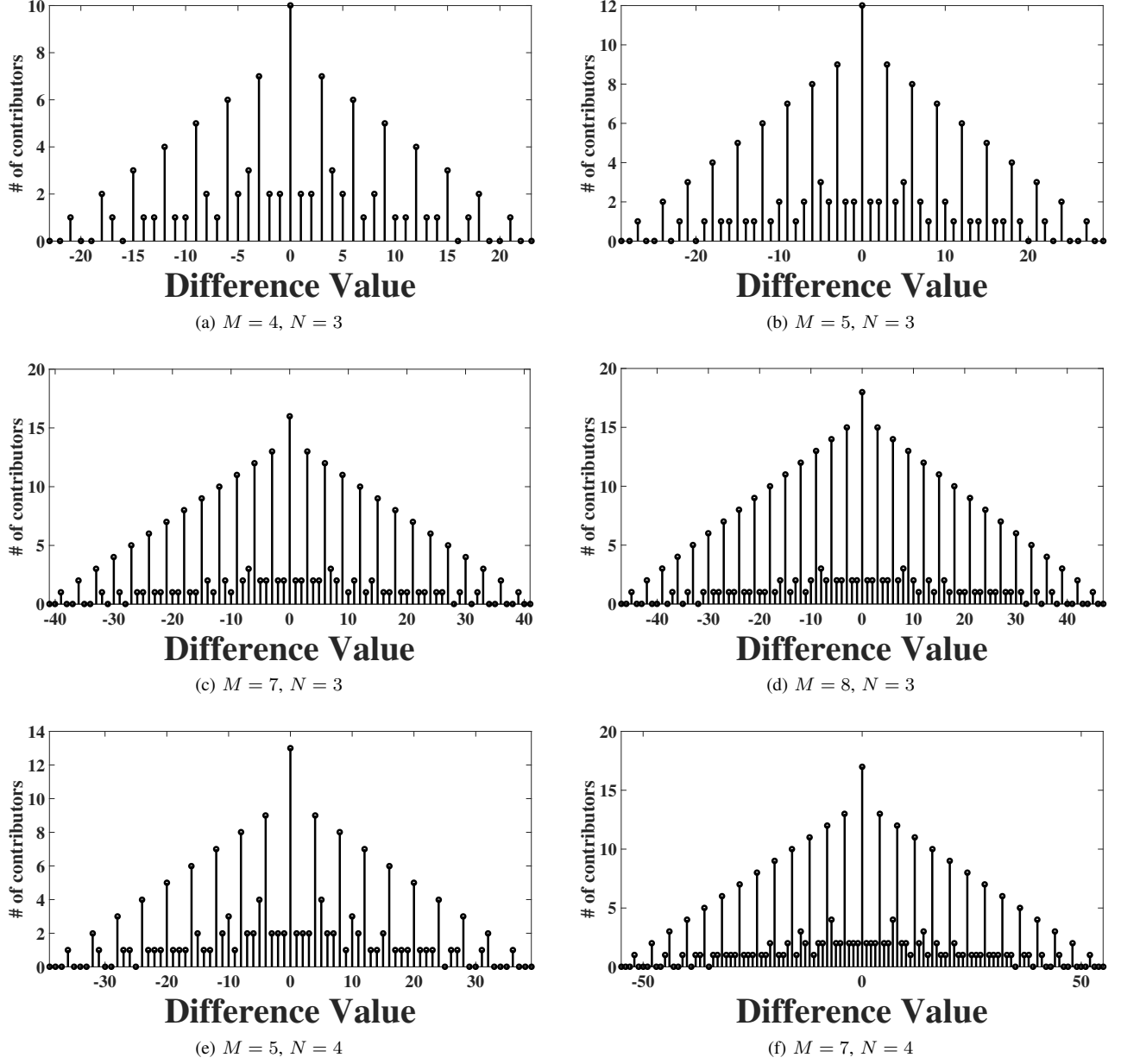
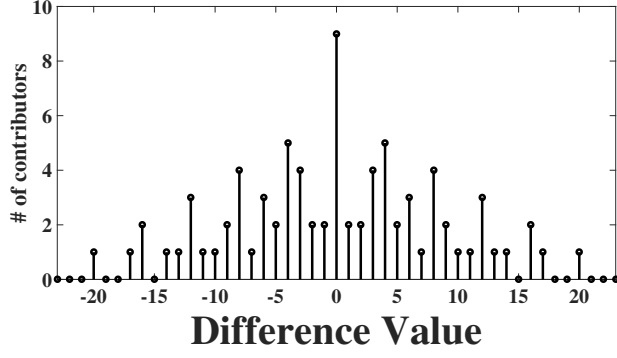
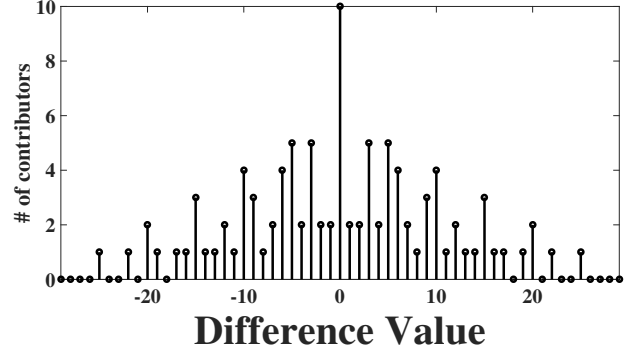
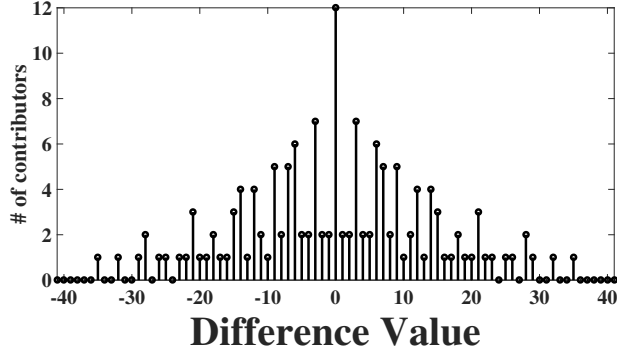
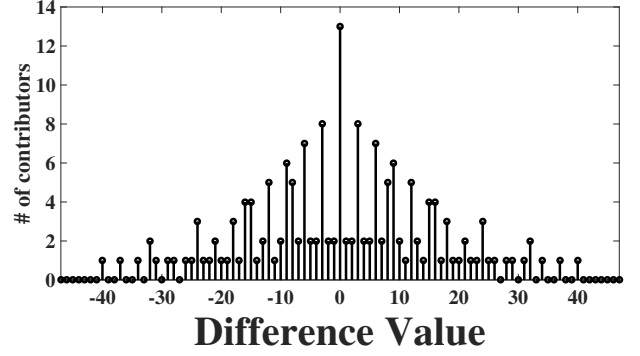
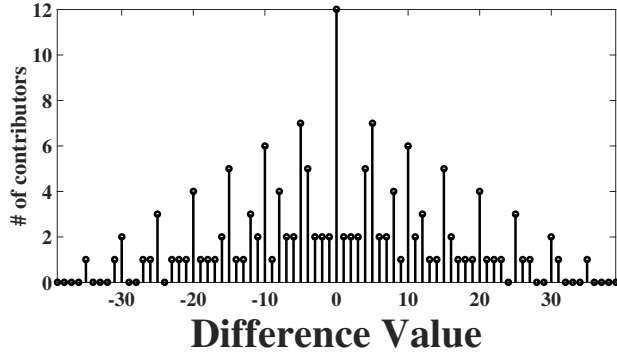
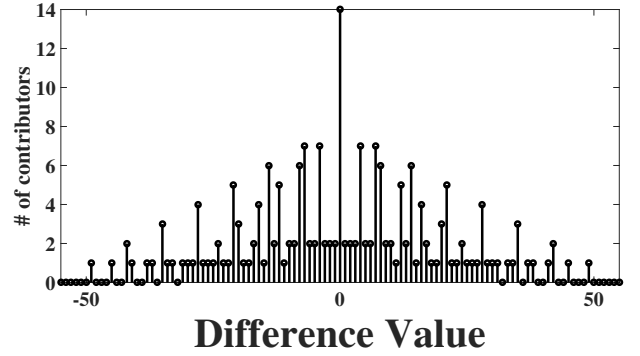


Fig. 5: Weight function: $M > N$.

the continuous difference set and for the prototype co-prime period. The reason for investigating it over the prototype co-prime period is because the initial motivation for the extension was to fill the holes in the region $[-MN + 1, MN - 1]$. The closed-form expression for the weight function of the extended co-prime array denoted by $z_{ef}(l)$, $z_{ec}(l)$ and $z_{ep}(l)$, for the three cases mentioned above, is given by equations (1)-(3) respectively. It may be noted that in this paper f , c and p will be used to represent the entire/full, continuous and the prototype range respectively.

$$\begin{aligned}
 z_{ef}(l) = & \underbrace{\sum_{n=-(N-1)}^{N-1} (N - |n| + 1) \delta(l - Mn)}_{A_f} \\
 & + \underbrace{\sum_{m=-(2M-1)}^{2M-1} (2M - |m|) \delta(l - Nm)}_{B_f} \\
 & + \underbrace{\sum_{n=1}^{N-1} \sum_{m=1}^{M-1} 2\delta(l - (Mn - Nm)) - \delta(l)}_{C_f} \\
 & + \underbrace{\sum_{n=1}^{N-1} \sum_{m=M+1}^{2M-1} \delta(|l| - |Mn - Nm|) - \delta(l)}_{D_f}
 \end{aligned} \tag{1}$$

(a) $M = 3, N = 4$ (b) $M = 3, N = 5$ (c) $M = 3, N = 7$ (d) $M = 3, N = 8$ (e) $M = 4, N = 5$ (f) $M = 4, N = 7$ Fig. 6: Weight function: $M < N$.

$$\begin{aligned}
 z_{e_c}(l) = & \underbrace{\sum_{n=-(N-1)}^{N-1} (N - |n| + 1) \delta(l - Mn)}_{A_c} \\
 & + \underbrace{\sum_{m=-\lfloor \frac{MN+M-1}{N} \rfloor}^{\lfloor \frac{MN+M-1}{N} \rfloor} (2M - |m|) \delta(l - Nm)}_{B_c} \\
 & + \underbrace{\sum_{n=1}^{N-1} \sum_{m=1}^{M-1} 2\delta(l - (Mn - Nm)) - \delta(l)}_{C_c} \\
 & + \underbrace{\sum_{n=1}^{N-1} \sum_{m=M+1}^{\lfloor \frac{MN+M+(Mn-1)}{N} \rfloor} \delta(|l| - |Mn - Nm|) - \delta(l)}_{D_c}
 \end{aligned} \quad (2)$$

$$\begin{aligned}
 z_{e_p}(l) = & \underbrace{\sum_{n=-(N-1)}^{N-1} (N - |n| + 1) \delta(l - Mn)}_{A_p} \\
 & + \underbrace{\sum_{m=-(M-1)}^{M-1} (2M - |m|) \delta(l - Nm)}_{B_p} \\
 & + \underbrace{\sum_{n=1}^{N-1} \sum_{m=1}^{M-1} 2\delta(l - (Mn - Nm)) - \delta(l)}_{C_p} \\
 & + \underbrace{\sum_{n=1}^{N-1} \sum_{m=M+1}^{\lfloor \frac{MN+(Mn-1)}{N} \rfloor} \delta(|l| - |Mn - Nm|) - \delta(l)}_{D_p}
 \end{aligned} \quad (3)$$

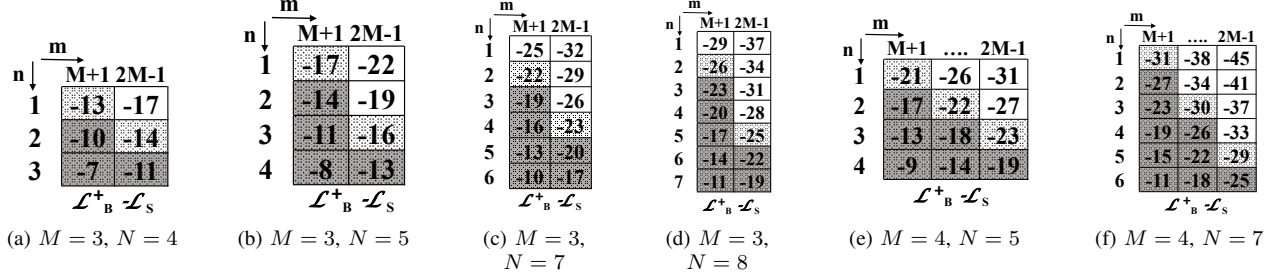


Fig. 7: Region for continuous range and co-prime period range of integers in set $\mathbf{L}_B^+ - \mathbf{L}_S : N > M$.

The expressions for z_{ef} , z_{ec} and z_{ep} are directly obtained from Proposition II. z_{ef} is a function over the entire difference set (f indicates full range). A_f is similar to A except for one additional contributor, B_f is similar to B with M replaced by $2M$ and C_f is equal to C (where A , B and C were described in [16]). D_f represents single contributors in the set \mathbf{L}_B^+ excluding the self differences. The use of $|l|$ in $\delta(|l| - |Mn - Nm|)$ is due to the fact that $(Mn - Nm)$ generates values in $\mathbf{L}_B^+ - \mathbf{L}_S$ which are all negative.

The continuous range of the extended array limits the self differences in the set \mathbf{L}_{SN}^+ to Nm , where $m \in [0, \lfloor \frac{MN+M-1}{N} \rfloor]$, and leads to equation B_c . C_c is same as C_f and hence C .

The prototype co-prime range is given by $\pm(MN - 1)$, hence $A_p = A_c = A_f$ and $C_p = C_c = C_f = C$. Since $m \in [0, M - 1]$, we obtain equation B_p .

The range for equations D_c and D_p cannot be directly inferred and hence, to provide an insight into its formulation consider Fig. 7 and 8, which displays $\mathbf{L}_B^+ - \mathbf{L}_S$ for different values of (M, N) . Fig. 8 represents the set when $M > N$, while Fig. 7 considers scenarios in which $M < N$. Note that all combinations of (M, N) , i.e., (odd, even), (even, odd) and (odd, odd) are considered. The dotted boxes represent the elements in the continuous range while the shaded boxes represent the prototype range.

For $M > N$, $\mathbf{L}_B^+ - \mathbf{L}_S$ has $n \in [1, N - 1]$ and the lower limit of m is $M + 1$ while the upper limit is given by (4) and (5) for the continuous and prototype co-prime range respectively.

$$\begin{aligned} Mn - Nm &\geq -(MN + M - 1) \\ m &\leq \left\lfloor M + \frac{M}{N} + \frac{1}{N}(Mn - 1) \right\rfloor \end{aligned} \quad (4)$$

$$\begin{aligned} Mn - Nm &\geq -(MN - 1) \\ m &\leq \left\lfloor M + \frac{1}{N}(Mn - 1) \right\rfloor \end{aligned} \quad (5)$$

For $N > M$, $\mathbf{L}_B^+ - \mathbf{L}_S$ has $m \in [M + 1, 2M - 1]$ and the upper limit of n is $N - 1$ while the lower limit is given by equation (6) and (7) for the continuous and co-prime range respectively.

$$\begin{aligned} Mn - Nm &\geq -(MN + M - 1) \\ n &\geq \left\lceil -(N + 1) + \frac{1}{M}(Nm + 1) \right\rceil \end{aligned} \quad (6)$$

$$\begin{aligned} Mn - Nm &\geq -(MN - 1) \\ n &\geq \left\lceil -N + \frac{1}{M}(Nm + 1) \right\rceil \end{aligned} \quad (7)$$

Equations (2) and (3) are presented for the case when $M > N$. Fig. 7 ($N > M$) has the same elements in the continuous and co-prime range as that in Fig. 8 ($M > N$), which implies that the equations derived for $M > N$ holds true for $N > M$. The correlogram bias window is described in [16] where $w_u(l)$ and $w_b(l)$ represent the window for the case when an unbiased and biased autocorrelation estimator is used to obtain the correlogram spectral estimate respectively. It may be noted that $w_u(l)$ is a rectangular window for the continuous set and the prototype co-prime period. However, it has zeros at locations corresponding to the holes for the entire difference set. The Fourier transform of the windows $w_u(l)$ and $w_b(l)$ represent the bias that perturbs the true spectrum and is denoted by $W_u(e^{j\omega})$ and $W_b(e^{j\omega})$ respectively. The bias $W_u(e^{j\omega})$ is given by (8) for the entire set with $L = 2MN - 1$, while (9) represents the bias for the continuous and prototype range where L is equal to $MN + M - 1$ and $MN - 1$ respectively.

$$\begin{aligned} W_u(e^{j\omega}) &= 2\cos\left(\frac{\omega MN}{2}\right) \frac{\sin\left(\frac{\omega M(N-1)}{2}\right)}{\sin\left(\frac{\omega M}{2}\right)} \\ &+ 2\cos(\omega MN) \frac{\sin\left(\frac{\omega N(2M-1)}{2}\right)}{\sin\left(\frac{\omega N}{2}\right)} + 1 \end{aligned} \quad (8)$$

$$\begin{aligned} &+ [1 + 2\cos(\omega MN)] \frac{\sin\left(\frac{\omega M(N-1)}{2}\right) \sin\left(\frac{\omega N(M-1)}{2}\right)}{\sin\left(\frac{\omega M}{2}\right) \sin\left(\frac{\omega N}{2}\right)} \\ W_u(e^{j\omega}) &= \frac{\sin\left(\frac{\omega(2L+1)}{2}\right)}{\sin\left(\frac{\omega}{2}\right)} \end{aligned} \quad (9)$$

Equation (9) is obvious since it is the Fourier transform of a rectangular function, while the proof for (8) is given here.

Proof: The closed-form expression for the weight function of the unbiased autocorrelation estimator for the entire difference set of an extended co-prime array is given below:

$$\begin{aligned} w_u(l) &= \sum_{m=1}^{2M-1} \delta(|l| - Nm) + \sum_{n=1}^{N-1} \sum_{m=1}^{M-1} \delta(l - (Mn - Nm)) + \\ &\delta(l) + \sum_{n=1}^{N-1} \delta(|l| - Mn) + \sum_{n=1}^{N-1} \sum_{m=M+1}^{2M-1} \delta(|l| + (Mn - Nm)) \end{aligned}$$

Note that the first four terms are same as that of the prototype co-prime array [16], except that the upper limit of the first

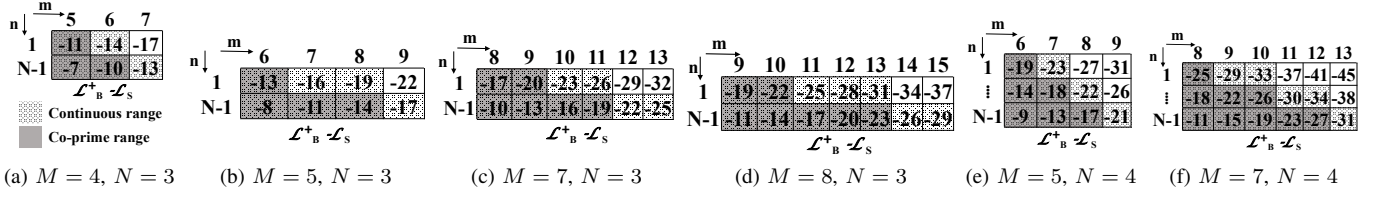


Fig. 8: Region for continuous range and co-prime period range of integers in set $\mathcal{L}_B^+ - \mathcal{L}_S : M > N$.

$$W_{b_f}(e^{j\omega}) = \frac{1}{s_b} \left\{ \left| \frac{\sin(\frac{\omega MN}{2})}{\sin(\frac{\omega M}{2})} \right|^2 + \frac{\sin(\frac{\omega M(2N-1)}{2})}{\sin(\frac{\omega M}{2})} + \left| \frac{\sin(\omega MN)}{\sin(\frac{\omega N}{2})} \right|^2 + 2(1 + \cos(\omega MN)) \frac{\sin(\frac{\omega M(N-1)}{2}) \sin(\frac{\omega N(M-1)}{2})}{\sin(\frac{\omega M}{2}) \sin(\frac{\omega N}{2})} - 2 \right\} \quad (10)$$

$$W_{b_c}(e^{j\omega}) = \frac{1}{s_b} \left\{ \left| \frac{\sin(\frac{\omega MN}{2})}{\sin(\frac{\omega M}{2})} \right|^2 + \frac{\sin(\frac{\omega M(2N-1)}{2})}{\sin(\frac{\omega M}{2})} + \left| \frac{\sin(\frac{\omega N(M + \lfloor \frac{M-1}{N} \rfloor + 1)}{2})}{\sin(\frac{\omega N}{2})} \right|^2 + (M - \lfloor \frac{M-1}{N} \rfloor - 1) \frac{\sin(\frac{\omega N(2M+2\lfloor \frac{M-1}{N} \rfloor + 1)}{2})}{\sin(\frac{\omega N}{2})} \right. \\ \left. + 2 \frac{\sin(\frac{\omega M(N-1)}{2}) \sin(\frac{\omega N(M-1)}{2})}{\sin(\frac{\omega M}{2}) \sin(\frac{\omega N}{2})} + \sum_{n=1}^{N-1} 2 \cos(\omega(Mn - \frac{MN}{2} - \frac{N(\lfloor \frac{MN+M+(Mn-1)}{N} \rfloor + 1))}{2}) \frac{\sin(\frac{\omega N(\lfloor \frac{MN+M+(Mn-1)}{N} \rfloor - M)}{2})}{\sin(\frac{\omega N}{2})} - 2 \right\} \quad (11)$$

$$W_{b_p}(e^{j\omega}) = \frac{1}{s_b} \left\{ \left| \frac{\sin(\frac{\omega MN}{2})}{\sin(\frac{\omega M}{2})} \right|^2 + \frac{\sin(\frac{\omega M(2N-1)}{2})}{\sin(\frac{\omega M}{2})} + \left| \frac{\sin(\frac{\omega MN}{2})}{\sin(\frac{\omega N}{2})} \right|^2 + M \frac{\sin(\frac{\omega N(2M-1)}{2})}{\sin(\frac{\omega N}{2})} \right. \\ \left. + 2 \frac{\sin(\frac{\omega M(N-1)}{2}) \sin(\frac{\omega N(M-1)}{2})}{\sin(\frac{\omega M}{2}) \sin(\frac{\omega N}{2})} + \sum_{n=1}^{N-1} 2 \cos(\omega(Mn - \frac{MN}{2} - \frac{N(\lfloor \frac{MN+(Mn-1)}{N} \rfloor + 1))}{2}) \frac{\sin(\frac{\omega N(\lfloor \frac{MN+(Mn-1)}{N} \rfloor - M)}{2})}{\sin(\frac{\omega N}{2})} - 2 \right\} \quad (12)$$

term is $2M - 1$ in this case. The contribution of the last term to the bias is given by:

$$\sum_{l=-(L-1)}^{L-1} \sum_{n=1}^{N-1} \sum_{m=M+1}^{2M-1} \delta(|l| + (Mn - Nm)) e^{-j\omega l} \\ = 2 \cos(\omega MN) \frac{\sin(\frac{\omega M(N-1)}{2}) \sin(\frac{\omega N(M-1)}{2})}{\sin(\frac{\omega M}{2}) \sin(\frac{\omega N}{2})}$$

It may be noted that the identity $\sum_{m=M+1}^{2M-1} \alpha^m = \alpha^{M+1} \left[\frac{1-\alpha^{M-1}}{1-\alpha} \right]$ is used to arrive at the above equation. By combining the five terms, we get (8). The weight $w_u(l)$ and the bias $W_u(e^{j\omega})$ for $M = 4$ and $N = 3$ is given in Fig. 9. It is evident that the derived bias expressions match the simulated FFT of $w_u(l)$. The bias in this case is not positive and hence cannot guarantee a positive spectral estimate. This was also found to be true for the prototype co-prime and the Nyquist schemes when an unbiased autocorrelation estimator of fixed length is employed.

The bias window that perturbs the true spectrum when a biased autocorrelation estimator is employed in the correlogram method is given by (10)-(12) for the three cases in (1)-(3) respectively.

The proof can be derived by first deriving the Fourier transform of X_x (i.e. $\mathfrak{F}\{X_x\}$), where X is one of the elements in $\{A, B, C, D\}$ and x in $\{f, c, p\}$. It follows a similar procedure as in [16]. The weight function for the cases in Fig. 8 ($M > N$) and Fig. 7 ($N > M$) is shown in Fig. 5 and 6 respectively. The FFT of these weight functions is the bias

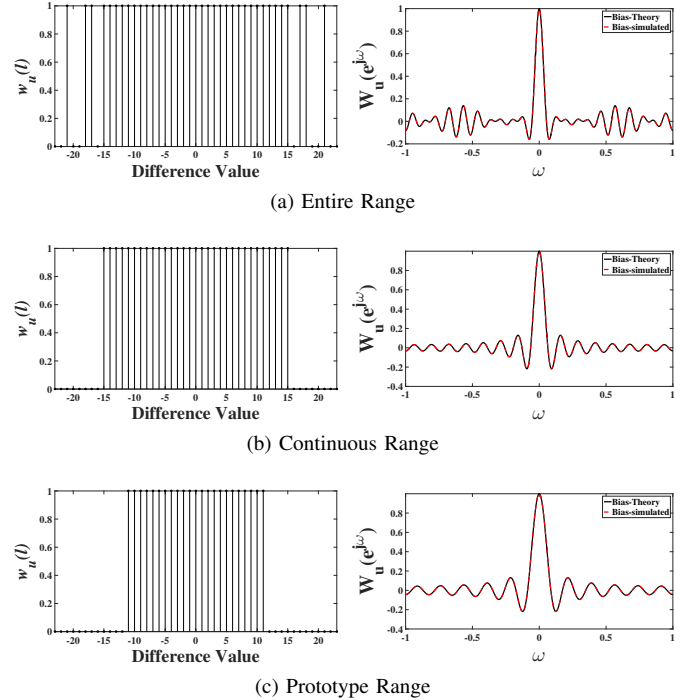


Fig. 9: Window $w_u(l)$ and its corresponding bias $W_u(e^{j\omega})$.

of the correlogram estimate for the entire, continuous and the prototype range (i.e. FFT of z_{ef} , z_{ec} and z_{ep}). These simulated results are compared with the derived bias equations in Fig. 10 for $M > N$ and for $N > M$. Each subplot in this figure

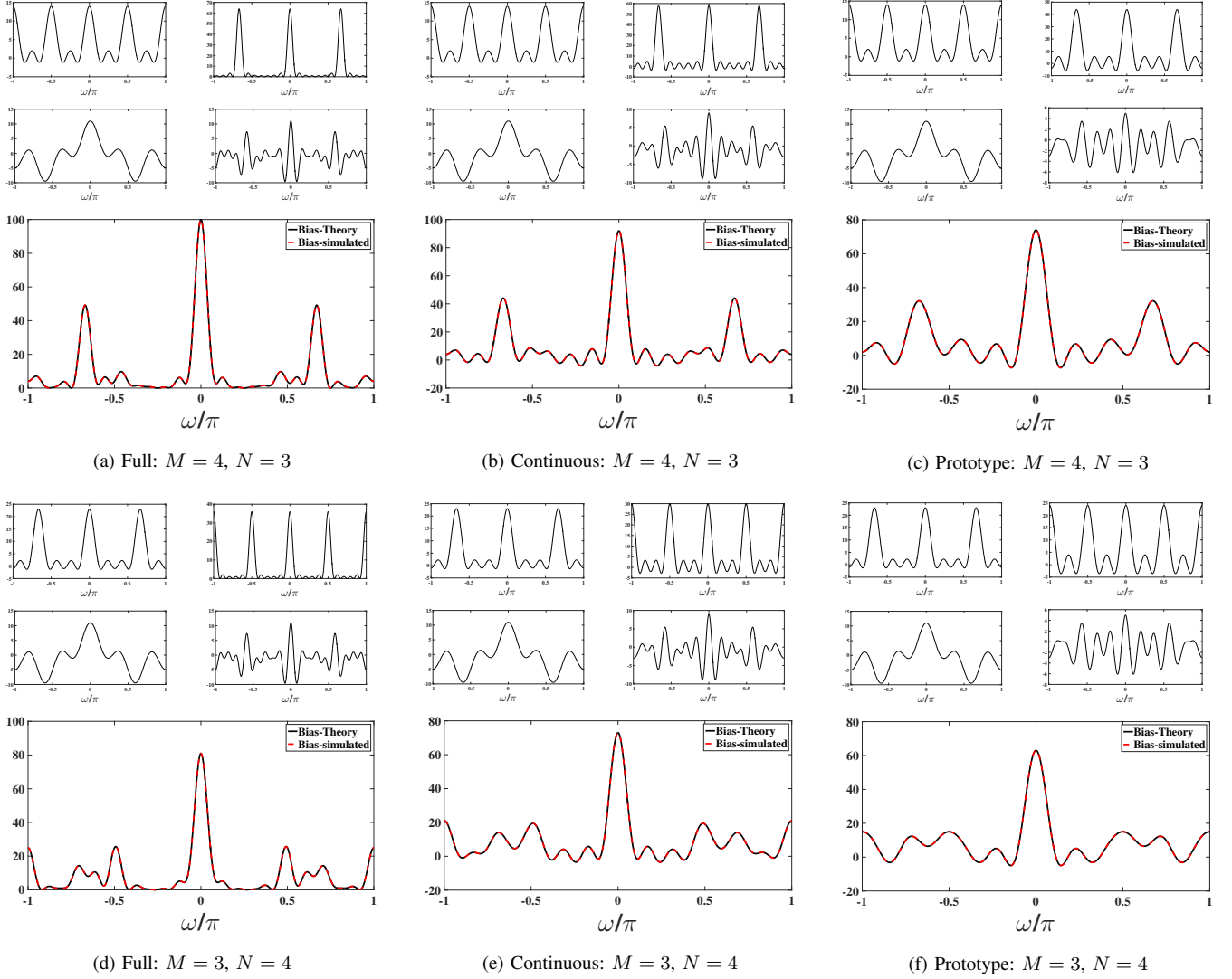


Fig. 10: Bias of the correlogram spectral estimate: $M > N$ (top), $N > M$ (bottom)

contains five images, and represent $\mathfrak{F}\{A_x\}$ (top-left), $\mathfrak{F}\{B_x\}$ (top-right), $\mathfrak{F}\{C_x\}$ (middle-left), $\mathfrak{F}\{D_x\}$ (middle-right) and overall bias $W_{b_x}(e^{j\omega})$ (bottom), where x denotes one of the elements $\{f, c, p\}$. It is evident that the derived equations in all the cases considered match the simulated results. Noted that the derived equations are valid for $M > N$ as well as $N > M$. Though the equations are valid for M greater than N and vice versa, the effect on the bias is not the same. This aspect is analyzed so as to provide an insight into the choice for array extension from a bias perspective. To address this issue a comparison between the bias for $M > N$ and $N > M$ is provided in Fig. 11. The black triangle represents the main-lobe and side-lobe peak when $M > N$ and the red circle represents these peaks when $N > M$. The peak side-lobe is detected using the *findpeaks* command in matlab, and is shown in the range $[-\pi, 0]$. The main-lobe peak is plotted using the formula obtained by substituting $\omega = 0$ in (10)-(12), and is given by (13)-(15) for the entire, continuous and prototype

sets:

$$W_{b_f}(e^{j0}) = (2M + N - 1)^2 \quad (13)$$

$$W_{b_c}(e^{j0}) = (M + \lfloor \frac{M-1}{N} \rfloor + 1)^2 + (M + N)^2 + M^2 - 3M - 3\lfloor \frac{M-1}{N} \rfloor - 2\lfloor \frac{M-1}{N} \rfloor^2 - 2 + \sum_{i=1}^{N-1} 2\lfloor \frac{M + Mi - 1}{N} \rfloor \quad (14)$$

$$W_{b_p}(e^{j0}) = 3M^2 + N^2 - 3M + 2MN - 1 + \sum_{i=1}^{N-1} 2\lfloor \frac{Mi - 1}{N} \rfloor \quad (15)$$

The relative amplitude (R) between the main lobe peak P_m and side-lobe peak P_s is given by $R = (P_m - P_s)/P_m$, and is computed for few examples in Table II. It is evident that R is large when $N > M$ for all the three cases, viz. entire, continuous and prototype range. The set-up considered in this paper extends the second array with inter-element spacing

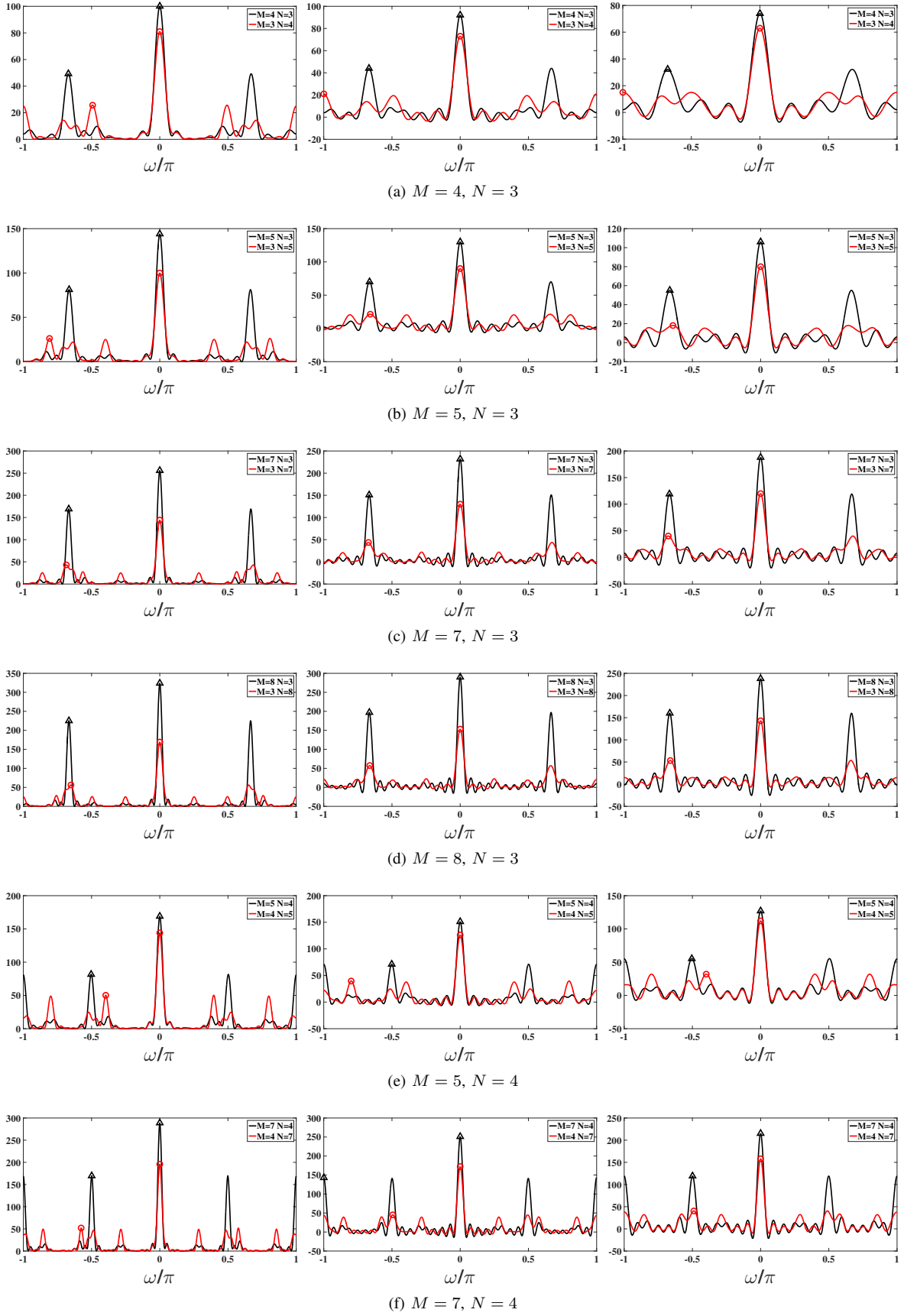


Fig. 11: Comparison between the bias for $M > N$ and $M < N$: Entire (left), continuous (middle) and prototype (right) range.

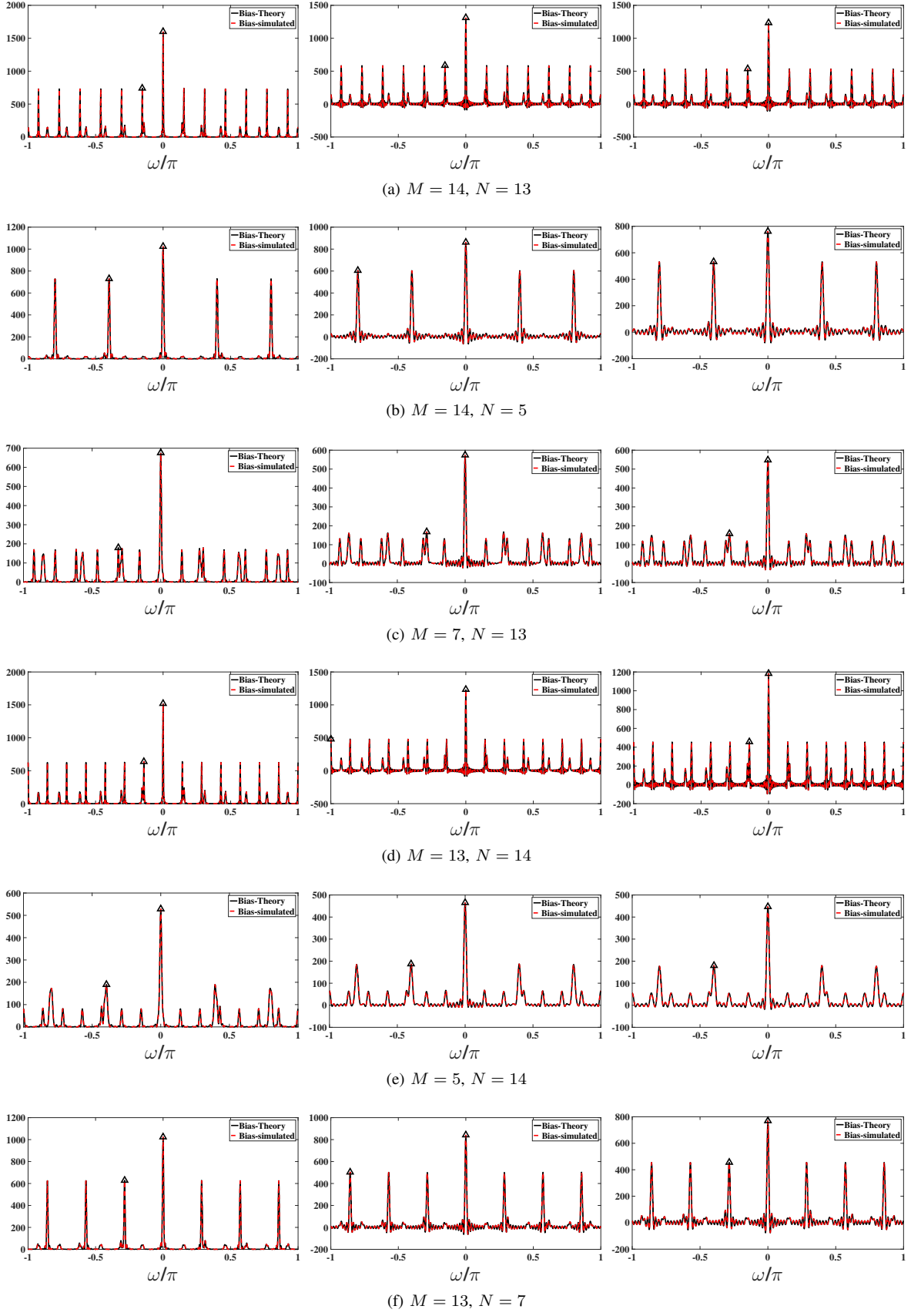


Fig. 12: Choice of (M, N) for the extended co-prime array: Entire (left), continuous (middle) and prototype (right) range.

TABLE II: Relative distance between main-lobe and side-lobe peak: A comparison between $M > N$ and $N > M$

M	N	$M > N$			$N > M$ (interchange M and N)		
		f	c	p	f	c	p
4	3	0.508	0.521	0.565	0.683	0.712	0.762
5	3	0.436	0.461	0.481	0.737	0.764	0.774
7	3	0.339	0.349	0.367	0.701	0.664	0.665
8	3	0.305	0.320	0.328	0.667	0.626	0.626
5	4	0.516	0.529	0.564	0.651	0.685	0.714
7	4	0.413	0.430	0.446	0.735	0.737	0.744

TABLE III: Relative distance between main-lobe and side-lobe peak: A comparison between $M > N$ and $N > M$

(M,N)		(14,13)	(14,5)	(7,13)	(13,14)	(5,14)	(13,7)
Relative Distance	f	0.537	0.287	0.734	0.580	0.641	0.387
	c	0.553	0.297	0.708	0.610	0.597	0.403
	p	0.566	0.302	0.710	0.614	0.597	0.408

Nd. In general, it implies that the array with larger inter-element spacing should be extended. It may also be noted from Fig. 11 that the bias is positive only for the case when the entire difference set is employed. Therefore, while using the continuous or the prototype range, a window function would have to be used to guarantee a valid positive power spectrum. Another important observation is that the main-lobe width is the least for the entire set, high for the continuous set and highest for the prototype set. Therefore, the spectral resolution will be high when the entire set is used, and least for the prototype co-prime range.

Despite the detailed analysis, what is the optimum value of M and N , is a question that still remains unanswered. For the prototype co-prime array it was observed that small consecutive integers were a good choice to maximize the relative amplitude between the main lobe and side-lobe peaks. For this choice, the side-lobe peaks were approximately of the same height [16]. Similarly, we wish that the extended co-prime array has side-lobe peaks that are approximately of the same height (contributed by both the sub-arrays). Fig. 12 shows the bias for consecutive values of M and N , as well as for the case when M is approximately half the value of N and vice versa. Table III compares the relative distance between the main-lobe and side-lobe peaks for the cases considered in Fig 12. In addition to the fact that N should be greater than M , it is now evident that consecutive values of M and N are not an optimum choice for maximizing the distance between the main-lobe and peak side-lobe. $M \approx \frac{N}{2}$ seems to be an optimum choice for the extended co-prime array.

VI. VARIANCE ANALYSIS

The variance of the extended co-prime array is analyzed along similar lines as that of the prototype and multiple period co-prime array [16]. We assume that $x(n)$ is a circular complex gaussian white process with zero mean and variance σ^2 [19] [20]. The expected value of the extended co-prime array-based correlogram for this process is given by:

$$\mathbb{E}\{\hat{P}(e^{j\omega})\} = \sum_l w_b(l) \sigma^2 \delta(l) e^{-j\omega l} = w_b(0) \sigma^2 = P(e^{j\omega})$$

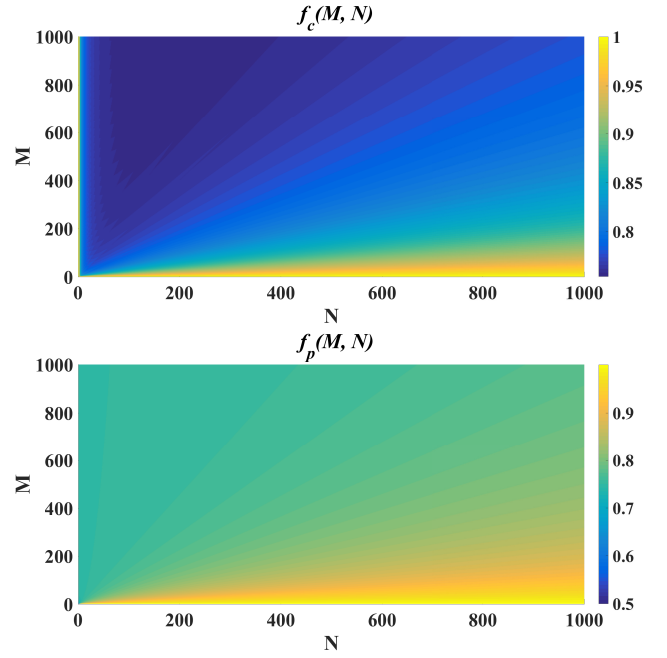


Fig. 13: Variance for the continuous and prototype range: $f_c(M, N)$ and $f_p(M, N)$

where s_b is assumed to be $2M + N - 1$, and hence gives $w_b(0) = 1$. Therefore, the expected value matches the true spectrum. The covariance of the correlogram estimate for the extended co-prime array is given by the bias equations (10), (11) and (12) when ω is replaced by $\omega_1 - \omega_2$ (as noted in [16]) for the entire, continuous and prototype co-prime range respectively. The scale factor is $\frac{\sigma^2}{s_b^2}$ (instead of $\frac{1}{s_b}$).

For the case when $(\omega_1 - \omega_2) = 0$, we have, $Cov\{\hat{P}_f(e^{j\omega_1})\hat{P}_f(e^{j\omega_2})\} = \sigma^4$. Therefore, the estimate using the entire difference set is not consistent. The variance of the correlogram estimate for the continuous and prototype range is:

$$\begin{aligned} Cov\{\hat{P}_c(e^{j\omega_1})\hat{P}_c(e^{j\omega_2}) | (\omega_1 - \omega_2) = 0\} &= \sigma^4 f_c(M, N) \\ Cov\{\hat{P}_p(e^{j\omega_1})\hat{P}_p(e^{j\omega_2}) | (\omega_1 - \omega_2) = 0\} &= \sigma^4 f_p(M, N) \end{aligned}$$

where $f_c(M, N)$ and $f_p(M, N)$ are given by (14) and (15) respectively, scaled by $\frac{1}{s_b^2}$. These functions are shown in Fig. 13 for $1 \leq M, N \leq 1000$ and includes (M, N) pairs that are not co-prime.

VII. COMPUTATIONAL COMPLEXITY

The number of multiplications and additions required for the prototype co-prime array-based autocorrelation estimation was derived in [16], [21] for the entire difference set. The continuous range was not considered. We provide the number of multiplications and additions for the continuous range denoted by C_M and C_A respectively in (16) for $M > N$. Since the autocorrelation function is symmetric, the complexity is derived for $l \in [0, L]$ where $L = M + N - 1$. $z_c(l)$ is the weight function of the prototype co-prime array for the continuous range and was derived in [16]. The total number

$$C_M = \sum_{l=0}^{M+N-1} z_c(l) = (2M + 4N - 4) + \left(\left\lfloor \frac{M+N-1}{N} \right\rfloor + 1 \right) \left(M - \left\lfloor \frac{M+N-1}{2} \right\rfloor - 2 \right)$$

$$C_A = \sum_{l \in \{l | z_c(l) > 1\}} [z_c(l) - 1] = \sum_{l=0}^{M+N-1} z_c(l) - \sum_{\{l | z_c(l) \geq 1\}} 1 = (M + 3N - 4) + \left(\left\lfloor \frac{M+N-1}{N} \right\rfloor + 1 \right) \left(M - \left\lfloor \frac{M+N-1}{2} \right\rfloor - 2 \right) \quad (16)$$

$$C_{M_f} = \frac{(2M + N)(2M + N - 1)}{2} \text{ and } C_{A_f} = \frac{4M^2 + N^2 + MN - 3M - 1}{2} \quad (17)$$

$$C_{M_c} = \sum_{l=0}^{MN+M-1} z_{e_c}(l) = \frac{N^2 + 3M^2 + 2MN + N + M + \lfloor \frac{M-1}{N} \rfloor (2M - 1 - \lfloor \frac{M-1}{N} \rfloor)}{2} + \sum_{n=1}^{N-1} \left\lfloor \frac{M + Mn - 1}{N} \right\rfloor - 1$$

$$C_{A_c} = \sum_{l=0}^{MN+M-1} z_{e_c}(l) - \sum_{\{l | z_{e_c}(l) \geq 1\}} 1 = \frac{N^2 + 3M^2 + N - M + \lfloor \frac{M-1}{N} \rfloor (2M - 1 - \lfloor \frac{M-1}{N} \rfloor)}{2} + \sum_{n=1}^{N-1} \left\lfloor \frac{M + Mn - 1}{N} \right\rfloor - 1 \quad (18)$$

$$C_{M_p} = \frac{N^2 + 3M^2 + N - M + 2MN}{2} + \sum_{n=1}^{N-1} \left\lfloor \frac{Mn - 1}{N} \right\rfloor - 1 \text{ and } C_{A_p} = \frac{N^2 + 3M^2 + N - M}{2} + \sum_{n=1}^{N-1} \left\lfloor \frac{Mn - 1}{N} \right\rfloor - 1 \quad (19)$$

of multiplications required is the summation of the weight function while the adders is given by the summation of the weights minus one at each difference value.

Next, we consider the computational complexity for the extended co-prime array. Let C_{M_x} and C_{A_x} denote the number of multiplications and additions required for autocorrelation estimation for the extended co-prime array respectively, where $x = \{f, c, p\}$ for the full, continuous and prototype range. The complexity is given by (17)-(19) for the entire, continuous and prototype range respectively and is derived using the corresponding weights z_{e_f} , z_{e_c} , and z_{e_p} .

VIII. NUMERICAL SIMULATIONS

Simulations are performed on a temporal signal model described in [7], [16]. The first step is to estimate the autocorrelation using the combined set. Next take the Fourier transform of the autocorrelation estimate to obtain the correlogram spectral estimate. Repeat this for L snapshots and compute the average correlogram. It may be noted that instead of calculating the correlogram using the autocorrelation, the Fourier transform of the acquired signal with zeros inserted at the holes (missing difference values) can be calculated, i.e. Periodogram. The entire difference range is considered here, since it guarantees a valid power spectrum (Refer [16]). We demonstrate the results for snapshots, $L = 10$. Fig. 14 and Fig. 15 demonstrates single peak estimation for different values of (M, N) . Several spurious peaks are observed. Note that $M \approx \frac{N}{2}$ seems to be a good choice. Furthermore, $(M, N) = (3, 7)$ or $(3, 8)$ works better.

Next, consider Fig. 16 and 17 for the estimation of three spectral peaks. Most of the examples considered here, have spurious peaks. $(M, N) = (3, 7)$ seems to be a good choice. Based on the analysis in this paper, we have the following thoughts:

- 1) On the basis of the bias window expression and the examples considered, we find that $M \approx \frac{N}{2}$ seems to be a good choice to reduce the side-lobes for the extended co-prime arrays.

- 2) The simulation results indicate that all values of $M \approx \frac{N}{2}$ will not work. For example, we find lower valued integer, i.e. $(M, N) = (3, 7)$ to be good.
- 3) Since the correlogram spectral estimate is the convolution of the bias window with the true spectrum (in a statistical sense), we conclude that the accuracy will also depend on the signal model. For example, $(M, N) = (3, 8)$ works for single peak estimation in Fig. 15 but fails for three peak estimation in Fig. 17.

In the next section, concluding remarks and possible questions for future research are considered.

IX. CONCLUSION

The fundamentals of the extended co-prime array was developed from a difference set perspective. The closed-form expression for the weight function and the bias of the correlogram spectral estimate is provided. This was derived for the entire difference set, continuous set and the set containing difference values in the prototype co-prime range. Simulations validate the correctness of the derived equations for all the three cases. The bias equations derived are valid for $M > N$ as well as $N > M$. However, it was found that the choice of $N > M$ provided a large relative amplitude between the main lobe and the side-lobe peaks. Since the structure assumed in this paper extends the array with inter-element spacing Nd , it can be concluded that the array with larger inter-element spacing should be extended. Furthermore, $M \approx \frac{N}{2}$ seems to be a good choice. We also analyze the variance of the correlogram estimate, and derive the number of multiplications and additions required for autocorrelation estimation. Low latency spectral estimation is demonstrated using the correlogram method.

The bias window expression describes the distortion in the estimate. This throws up several challenges which needs further investigation. For example, can the bias distortion be reduced? What could be the ways to achieve this? In addition, other spectral estimation methods can be investigated. Several applications can be explored for low latency estimation along similar lines.

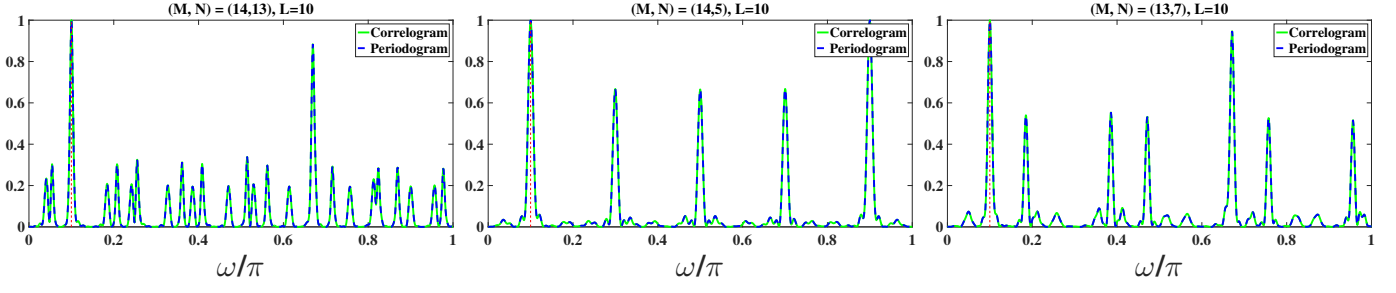


Fig. 14: Simulation results for spectral estimation (1 peak) with number of snapshots $L = 10$: (M, N) is $(14, 13)$, $(14, 5)$, $(13, 7)$.

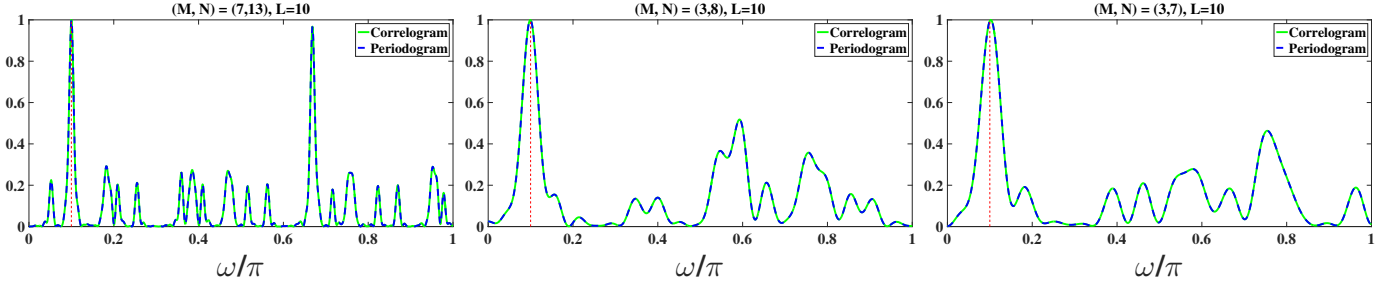


Fig. 15: Simulation results for spectral estimation (1 peak) with number of snapshots $L = 10$: (M, N) is $(7, 13)$, $(3, 8)$, $(3, 7)$.

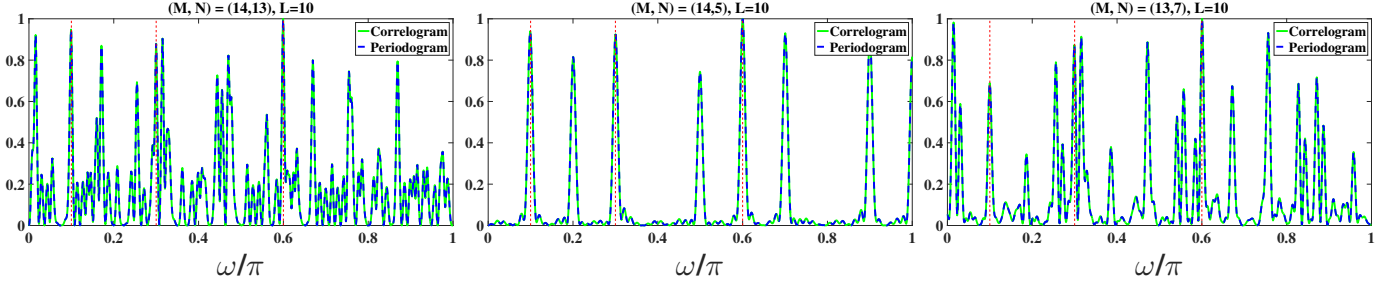


Fig. 16: Simulation results for spectral estimation (3 peaks) with number of snapshots $L = 10$: (M, N) is $(14, 13)$, $(14, 5)$, $(13, 7)$.

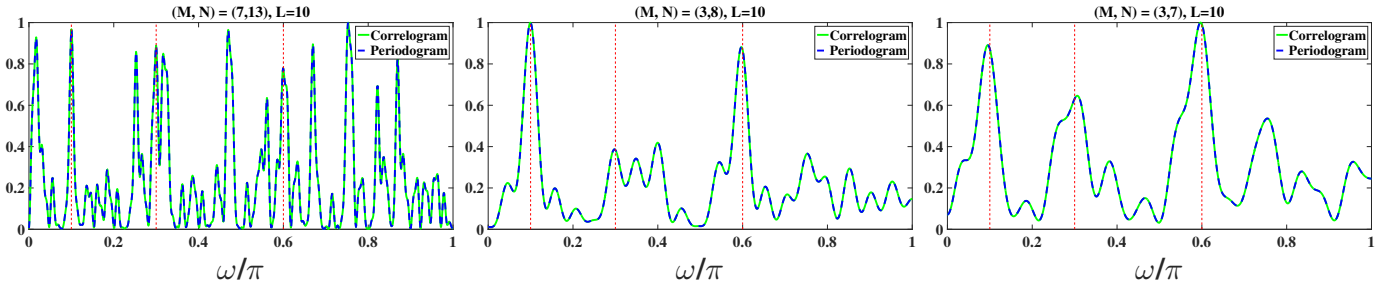


Fig. 17: Simulation results for spectral estimation (3 peaks) with number of snapshots $L = 10$: (M, N) is $(7, 13)$, $(3, 8)$, $(3, 7)$.

REFERENCES

- [1] P. P. Vaidyanathan and P. Pal, "Sparse sensing with co-prime samplers and arrays," *IEEE Trans. Signal Process.*, vol. 59, no. 2, pp. 573–586, Feb. 2011.
- [2] Y. D. Zhang, M. G. Amin, and B. Himed, "Sparsity-based DoA estimation using co-prime arrays," in *2013 IEEE International Conference on Acoustics, Speech and Signal Processing*, May 2013, pp. 3967–3971.
- [3] C. Zhou, Y. Gu, Y. D. Zhang, Z. Shi, T. Jin, and X. Wu, "Compressive sensing-based coprime array direction-of-arrival estimation," *IET Communications*, vol. 11, pp. 1719–1724(5), August 2017.
- [4] Z. Cheng, Y. Zhao, H. Li, and P. Shui, "Two-dimensional DoA estimation algorithm with co-prime array via sparse representation," *Electronics Letters*, vol. 51, pp. 2084–2086(2), December 2015.
- [5] F.-G. Yan, S. Liu, J. Wang, M. Jin, and Y. Shen, "Fast DoA estimation using co-prime array," *Electronics Letters*, vol. 54, pp. 409–410(1), April 2018.
- [6] S. Ren, Z. Zeng, C. Guo, and X. Sun, "Wideband spectrum sensing based on coprime sampling," in *22nd Int. Conf. Telecommunications*

- (ICT), 2015, pp. 348–352.
- [7] P. Pal and P. P. Vaidyanathan, “Soft-thresholding for spectrum sensing with coprime samplers,” in *IEEE Sensor Array and Multichannel Signal Processing Workshop (SAM)*. IEEE, 2014, pp. 517–520.
 - [8] P. P. Vaidyanathan and P. Pal, “System identification with sparse coprime sensing,” *IEEE Signal Processing Letters*, vol. 17, no. 10, pp. 823–826, Oct 2010.
 - [9] G. D. Martino and A. Iodice, “Passive beamforming with coprime arrays,” *IET Radar, Sonar and Navigation*, vol. 11, pp. 964–971(7), June 2017.
 - [10] K. Liu and Y. D. Zhang, “Coprime array-based robust beamforming using covariance matrix reconstruction technique,” *IET Communications*, vol. 12, pp. 2206–2212(6), October 2018.
 - [11] Y. Gu, C. Zhou, N. A. Goodman, W. Z. Song, and Z. Shi, “Coprime array adaptive beamforming based on compressive sensing virtual array signal,” in *2016 IEEE International Conference on Acoustics, Speech and Signal Processing (ICASSP)*, March 2016, pp. 2981–2985.
 - [12] U. V. Dias and S. Srirangarajan, “Co-prime sampling and cross-correlation estimation,” in *24th National Conference on Communications (NCC)*, Feb 2018.
 - [13] P. Pakrooh, L. L. Scharf, and A. Pezeshki, “Modal analysis using coprime arrays,” *IEEE Transactions on Signal Processing*, vol. 64, no. 9, pp. 2429–2442, May 2016.
 - [14] X. Huang, Z. Yan, S. Jing, H. Fang, and L. Xiao, “Co-prime sensing-based frequency estimation using reduced single-tone snapshots,” *Circuits, Systems, and Signal Processing*, vol. 35, no. 9, pp. 3355–3366, 2016.
 - [15] U. V. Dias and S. Srirangarajan, “Co-prime arrays and difference set analysis,” in *25th European Signal Processing Conference (EUSIPCO)*, 2017, pp. 961–965.
 - [16] U. V. Dias, “Sub-Nyquist co-prime sensing: Too little cannot belittle you,” Doctoral Thesis, Department of Electrical Engineering, Indian Institute of Technology Delhi, New Delhi, July 2020.
 - [17] P. Pal and P. P. Vaidyanathan, “Coprime sampling and the music algorithm,” in *2011 Digital Signal Processing and Signal Processing Education Meeting (DSP/SPE)*, Jan 2011, pp. 289–294.
 - [18] K. Han, P. Yang, and A. Nehorai, “Calibrating nested sensor arrays with model errors,” *IEEE Transactions on Antennas and Propagation*, vol. 63, no. 11, pp. 4739–4748, Nov 2015.
 - [19] P. Stoica and R. L. Moses, *Spectral Analysis of Signals*. Upper Saddle River, New Jersey: Pearson Prentice Hall, 2005, vol. 452.
 - [20] E. Axel. (2011, June 29) Lecture notes on nonparametric spectral estimation. [Online]. Available: <http://www.commsys.isy.liu.se/ADE/axell-notes.pdf>
 - [21] U. V. Dias and S. Srirangarajan, “Co-prime sampling jitter analysis,” in *25th European Signal Processing Conference (EUSIPCO)*, 2017, pp. 1180–1184.